13. The original selection experiment generated two high, two low, and two control strains (on which selection was not applied) (8). Breeding pairs for the experiment described here were derived from the first high and low strains (H_1 and L_1 respectively). DNA was extracted from spleens, diluted to a concentration of 10 ng/μl, and 50 ng used for each polymerase chain reaction (PCR). Murine microsatellites were selected that were known to distinguish C57LB/6J and BALB/cJ inbred strains (the progenitor strains for the original selection experiment) [W. F. Dietrich *et al.*, *Nat. Genet.* **7**, 220 (1994)]. Primers were obtained from Research Genetics. We tested 250 markers on the H_1 and L_1 inbred animals; 120 were found that differentiated these strains, and 84 were chosen to cover the genome with a maximum interval between markers of 30 centimorgans (cM). PCR analyses were performed in a volume of 15 μl in 96-well microtiter plates with 0.4 U of Taq polymerase, 4.0 μM deoxynucleotide triphosphate, 1× PCR buffer (Boehringer Mannheim), and 7.5 pmol of each primer. After an initial denaturation at 94°C for 4 min, reaction conditions were 30 cycles of 94°C for 45 s, 55°C for 1 min, and 72°C for 1 min. PCR products were resolved on 4% agarose gels.
14. E. S. Lander *et al.*, *Genomics* **1**, 174 (1987); S. Lincoln, M. Daly, E. Lander, *Mapping Genes Controlling Quantitative Traits with MAPMAKER/QTL 1.1* (Whitehead Institute, technical report, Cambridge, MA, 1992); A. Paterson *et al.*, *Nature* **335**, 721 (1988).
15. E. S. Lander and N. J. Schork, *Science* **265**, 2037 (1994).
16. J. Ott, *Analysis of Human Genetic Linkage* (Johns Hopkins Univ. Press, Baltimore, MD, 1991).
17. In addition, there is good agreement between the number of QTLs mapped for OFA and that predicted from Wright's formula for the likely number of effective factors (equivalent to the number of QTLs) [S. E. Wright, *Evolution and the Genetics of Populations: Genetic and Biometric Foundations* (Univ. of Chicago Press, Chicago, IL, 1968), pp. 373–420; W. E. Castle, *Science* **54**, 223 (1921)]. If this formula is applied to the phenotypic data from the F_2 intercross, there are 5.33 effective factors predicted for OFA. Furthermore, Wright's method also predicts a small number of QTLs for open-field defecation (2.23), in agreement with our findings.
18. When the four variables were subjected simultaneously to multivariate analysis of variance, significance levels at the marker closest to each putative QTL on the six chromosomes were as follows: chromosome 1, Wilks λ $F = 8.145$ (8 degrees of freedom), $P < 0.00001$; chromosome 4, $F = 3.601$, $P = 0.00004$; chromosome 12, $F = 4.748$, $P = 0.00001$; chromosome 15, $F = 5.531$, $P < 0.00001$; chromosome 17, $F = 2.570$, $P = 0.01$; chromosome 18, $F = 2.892$, $P = 0.004$.
19. F. S. Collins, *Nat. Genet.* **9**, 347 (1995).
20. M. A. Taylor, *Am. J. Psychiatry* **149**, 22 (1992); K. S. Kendler *et al.*, *Arch. Gen. Psychiatry* **50**, 952 (1993); W. Maier *et al.*, *ibid.*, **51**, 871 (1994); K. S. Kendler *et al.*, *ibid.* **49**, 716 (1992); R. B. Goldstein *et al.*, *ibid.* **51**, 383 (1994).
21. Supported in part by a grant from the U.S. National Institute on Drug Abuse (NIDA) (DA-05131). A.C.C. is supported in part by a Research Scientist Award from NIDA (DA-00197). J.F. is supported by the Wellcome Trust. We would like to acknowledge the support and encouragement of D. J. Weatherall and J. A. Todd.

24 February 1995; accepted 18 July 1995

Separation of Caveolae from Associated Microdomains of GPI-Anchored Proteins

Jan E. Schnitzer,* Deirdre P. McIntosh, Ann M. Dvorak, Jun Liu, Phil Oh

In situ coating of the surface of endothelial cells in rat lung with cationic colloidal silica particles was used to separate caveolae from detergent-insoluble membranes rich in glycosyl phosphatidylinositol (GPI)–anchored proteins but devoid of caveolin. Immunogold electron microscopy showed that ganglioside G_{M1}–enriched caveolae associated with an annular plasmalemmal domain enriched in GPI-anchored proteins. The purified caveolae contained molecular components required for regulated transport, including various lipid-anchored signaling molecules. Such specialized distinct microdomains may exist separately or together in the plasma membrane to organize signaling molecules and to process surface-bound ligands differentially.

Cholesterol and glycolipids self-associate in lipid bilayers to form organized compositional microdomains (*1*). GPI-anchored and other lipid-linked proteins may preferentially partition into glycolipid microdomains that are resistant to nonionic detergent solubilization (*2–5*). GPI-anchored proteins appear to be sorted into glycolipid, detergent-resistant "rafts" in the trans-Golgi network for polarized delivery to the cell surface by caveolin-rich smooth exocytotic carrier vesicles (*3, 5–8*). On the cell surface, they are thought to reside in smooth membrane invaginations known as caveolae (*9, 10*), which are apparently also rich in glycolipids, cholesterol, and caveolin (*7, 11–14*). Antibody cross-linking of cell surface glycolipids (*1*) and GPI-linked proteins (*15*) can increase sequestration into clusters and induce cell activation (*1, 16*), apparently through lipid-anchored nonreceptor tyrosine kinases (NRTKs) (*17*). Caveolae have been implicated not only in signaling but also in transport via endocytosis, transcytosis, and potocytosis (*14, 18–21*). The physiological functions of and interrelations between caveolae, detergent-resistant microdomains, and various lipid-anchored molecules remain undefined.

Department of Pathology, Harvard Medical School, Beth Israel Hospital, 99 Brookline Avenue, Boston, MA 02215, USA.

*To whom correspondence should be addressed.

To explore the relation between GPI-anchored proteins and caveolae under conditions that avoid potential influences of antibody effectors, cell culture (*22*), and contamination from intracellular compartments, we purified the plasma membranes of rat lung endothelial cells and then subfractionated them into specific microdomains. The rat lung vasculature was perfused in situ at 10° to 13°C with a suspension of cationic colloidal silica particles, which coated the luminal endothelial cell plasma membranes normally exposed to the circulating blood. This coating created a stable pellicle that specifically marked this membrane and enhanced its density, which allowed its purification from tissue homogenates by centrifugation (*13, 23*). The silica-coated membrane pellets (P) were enriched in endothelial cell surface markers, with little contamination from other tissue components (*13, 23*).

Caveolae attached on the cytoplasmic side of the plasma membranes, opposite to the silica coating, were stripped from these membranes by shearing during homogenization at 4°C in the presence of Triton X-100. They were then isolated by sucrose density gradient centrifugation to yield a homogeneous population of biochemically and morphologically distinct caveolar vesicles (Figs. 1 and 2). As with caveolae present on the endothelial cell surface in vivo (*7, 12, 24*), these purified caveolae (V) were enriched in caveolin, plasmalemmal Ca^{2+}-dependent adenosine triphosphatase, and the inositol 1,4,5-trisphosphate receptor (*13*). In contrast, other markers present amply in P, including angiotensin-converting enzyme, band 4.1, and β-actin, were almost totally excluded from V.

The purified caveolae were not rich in GPI-anchored proteins. First, detergent extraction studies performed on P revealed differences in the ability of various detergents to solubilize caveolin and 5′-nucleotidase (5′-NT). Caveolin was partially solubilized by β-octyl glucoside, CHAPS, deoxycholate, NP-40, and SDS (but not Triton X-100), whereas 5′-NT was rendered soluble only by SDS and deoxycholate (Fig. 1A). Second, like caveolin, 5′-NT and urokinase-plasminogen activator receptor (uPAR) were enriched in P relative to the starting rat lung homogenate (H) (Fig. 1C). However, unlike caveolin, these proteins were not enriched in V; they remained almost totally associated with the resedimented silica-coated membranes stripped of the caveolae (P−V) [which contain few, if any, remaining caveolae (*13*)]. More than 95% of the signal for caveolin was detected in V, with <4% remaining in P−V. Conversely, >95% of 5′-NT and uPAR remained in P−V, with <3% present in V. Thus, these GPI-anchored proteins were neither cou-

pled to caveolin nor concentrated in the isolated caveolin-enriched caveolae.

Other methodologies not based on the silica-coating technique have been developed for isolating low density, detergent-resistant membranes from a variety of cultured cells and tissues (*3–5, 25, 26*). By performing similar isolations with rat lung tissue as in (*26*), we showed, consistent with previous studies (*5, 25, 26*), that caveolin and GPI-anchored proteins (in this instance, 5′-NT) were both present in the isolated Triton X-100–insoluble membranes (TI) (Fig. 1B). In addition, differential detergent extraction studies were performed on TI. As expected (*3–5*), GPI-anchored proteins were solubilized effectively by β-octyl glucoside, CHAPS, deoxycholate, and SDS (*27*), different from the pattern of solubility for 5′-NT in P but similar to that for caveolin in P.

There has been a tendency to equate low density, Triton-insoluble membranes with caveolae (*5, 25, 26*). Electron microscopy of the V and TI membrane preparations revealed that V comprised a relatively homogeneous population of vesicles (≤100 nm) with the typical morphology of caveolae, whereas TI contained caveolae, linear membrane sheets, and many larger vesicles (≥150 nm) (Fig. 2). In many favorable cross sections, a characteristic flask-shaped caveola attached to a larger, spherical vesicle was apparent, suggesting that these two detergent-resistant membrane domains were associated with each other as a unit before fractionation in the membrane (Fig. 2, D and E).

Because the larger noncaveolar vesicles in TI contained the GPI-linked proteins (Fig. 3), it appeared that silica coating of the outer membrane surface altered the way in which the GPI-anchored proteins interacted with various detergents and thus prevented the separation of noncaveolar, detergent-resistant microdomains from the cell membranes. Cationic silica particles interact with the anionic cell surface to stabilize it against vesiculation or lateral rearrangement by immobilizing membrane molecules (*28*). Because the silica particles uniformly coated the cell surface but were rarely associated with or present inside the caveolae because of their size, it is likely (*13, 23*) that the plasma membrane was stabilized by being firmly attached on one side to most, if not all, nonvesiculated regions. This adherent pellicle would allow the caveolae on the opposite side of the membrane to be sheared away by homogenization, with little contamination from other membranes, including other detergent-resistant domains. Conversely, without silica coating, both caveolar and noncaveolar detergent-resistant membranes would be coisolated. In addition, without isolating the plasma membrane first, such preparations of cells and tissues would also contain intracellular detergent-insoluble caveolin-rich domains, such as those present in the trans-Golgi network (*3, 7*).

As a test, we increased the salt concentration during the isolation procedure, which reduced electrostatic interactions sufficiently to detach the plasma membrane from the silica pellicle in P and to allow the coisolation of caveolae with GPI-linked protein microdomains (*29*). More importantly, because the silica coating did indeed prevent the release of the detergent-insoluble membranes rich in GPI-anchored proteins, it was possible to isolate these domains separately from the caveolae. We incubated the silica-coated membranes already stripped of caveolae (P−V) with 2 M K_2HPO_4, followed by homogenization in Triton X-100 at 4°C. This procedure allowed the isolation by sucrose density gradient centrifugation of a membrane fraction (G) that contained vesicles of >150 nm in diameter with no apparent caveolae (*27*). G lacked caveolin but was enriched in several GPI-anchored proteins: 5′-NT, uPAR, and carbonic anhydrase (CA) (Fig. 1D). Little of these proteins remained behind in the resedimented membrane pellet (RP). The G/RP ratio ranged from ~3 for 5′-NT and uPAR to 12 for CA. Thus, distinct deter-

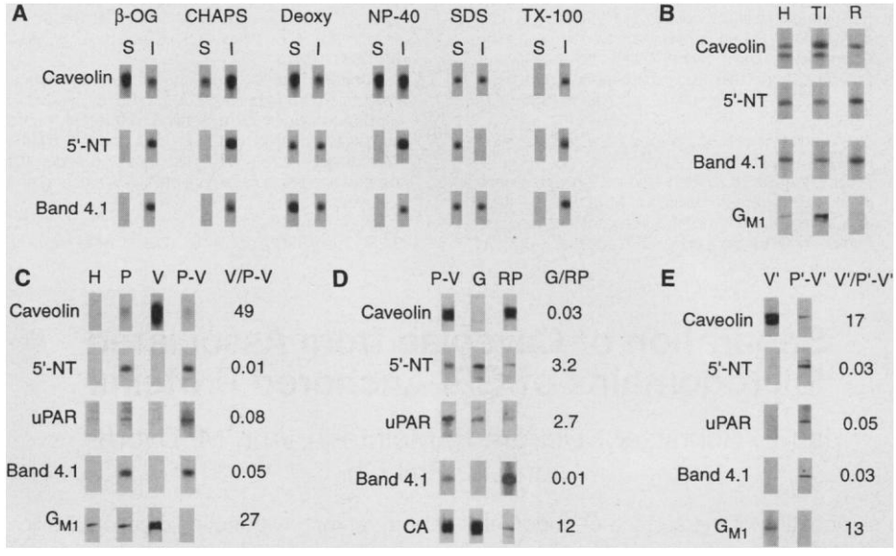

Fig. 1. Protein analysis of various membrane subfractions. (**A**) Differential detergent extraction performed on silica-coated endothelial cell membranes (P). Equal portions of resuspended P were incubated with rotation for 1 hour at 4°C with various detergents (β-OG, β-octylglucoside; Deoxy, sodium deoxycholate; TX-100, Triton X-100) before centrifugation at 13,000*g* for 2 hours. The soluble proteins (S) and the sedimented, insoluble proteins (I) were fractionated by SDS–polyacrylamide gel electrophoresis (10 μg per lane), transferred to nitrocellulose or Immobilon (Millipore) filters, and subjected to immunoblot analysis with equivalent amounts of specific antibodies for the indicated proteins and the appropriate ^{125}I-labeled secondary antibodies as described (*13, 20*). Other proteins tested included angiotensin-converting enzyme, which was solubilized by all of these detergents, and carbonic anhydrase, which was solubilized similarly to 5′-NT (*27*). (**B**) Coisolation of caveolin and 5′-NT in detergent-resistant membranes derived without silica coating. Proteins from rat lung homogenate (H), the Triton X-100–insoluble membranes isolated by sucrose density gradient centrifugation (TI), and the sedimented pellet (R) were subjected to immunoblot analysis as in (A), with the exception that the secondary antibodies were conjugated to horseradish peroxidase (HRP) and binding was detected with ECL chemiluminescent substrate (Amersham). (**C**) Lack of GPI-anchored proteins in the purified caveolae enriched in caveolin and ganglioside G_{M1}. Whole-lung homogenate (H), silica-coated luminal endothelial membranes (P), purified caveolae (V), and the resedimented silica-coated membranes after stripping of the caveolae (P−V) were subjected to immunoblot analysis as in (B). G_{M1} was detected not only by immunoblotting but also by direct blotting with HRP-conjugated cholera toxin. Ratios of the signals detected in V versus P−V are shown. (**D**) Separate isolation of the GPI-anchored protein microdomain from the silica-coated membranes. Immunoblot analysis was performed as in (B) with P−V, G [the detergent-resistant membranes derived from P−V after detaching the membrane from the silica (*46*)], and RP (the resedimented pellet of silica-containing material). The caveolin in P−V is equivalent to that seen in (C), representing the small residual signal after stripping of the caveolae (compare V and P−V), except that the exposure here is much longer. G_{M1} could not be detected in P−V [see (C)] nor, as expected, in G or RP (*27*). G is rich in GPI-linked proteins (5′-NT, uPAR, and CA) but lacks caveolin and G_{M1}. Control experiments performed identically but without high salt did not yield any detectable membranes in the sucrose gradient (*27*). (**E**) Immunoblot analysis of caveolae isolated without Triton X-100. Caveolae were purified without any exposure to detergent (*34*). These caveolae (V′) and the membrane stripped of them (P′−V′) were subjected to immunoblot analysis as in (B).

gent-resistant plasma membranes rich in GPI-anchored proteins but lacking caveolin could be isolated separately from the caveolae. Similar detergent-resistant membranes, consisting of large vesicles rich in GPI-anchored proteins but devoid of caveolin, have also been isolated from lymphocytes and neuroblastoma cells, both of which lack caveolae and do not express caveolin (*30*).

Although several studies that have examined the immunolocalization of GPI-anchored proteins in cultured cells have concluded that these proteins reside in caveolae (*9*), reexamination of the published electron micrographs reveals little gold labeling directly inside the caveolae. Almost all of this labeling is actually adjacent to the caveolae on the flat plasma membrane directly attached to, but not a part of, the neck of the caveolae. The small amount of labeling apparent inside the caveolae and the extent of clustering observed may be induced artifactually by antibody cross-linking (*15, 31*). In contrast, another lipid-anchored molecule, the cholera toxin–binding ganglioside G_{M1}, has been localized with gold labeling inside the caveolae (*11, 14*). The fractions isolated directly from the silica-coated membranes mimic these observations, with V containing >90% of G_{M1} (Fig. 1C). The remaining membrane devoid of caveolae lacked detectable G_{M1}, although it was rich in GPI-anchored proteins. Hence, G_{M1} was used as a caveolar marker.

The amounts of GPI-anchored proteins that partition into microdomains remain unclear, partially because antibody cross-linking can increase the clustering of GPI-linked proteins from ≤10 to >90%; again, gold immunolabeling is not in the caveolae but on the adjacent annular membrane (*15, 31*). Other studies that have examined membrane diffusion by fluorescence recovery after photobleaching have detected a larger fraction of GPI-anchored proteins (20 to 60%) present in an immobile fraction (*8, 32*). By examination of detergent solubility, we have detected similar percentages for the GPI-linked proteins in the detergent-resistant microdomains, suggesting

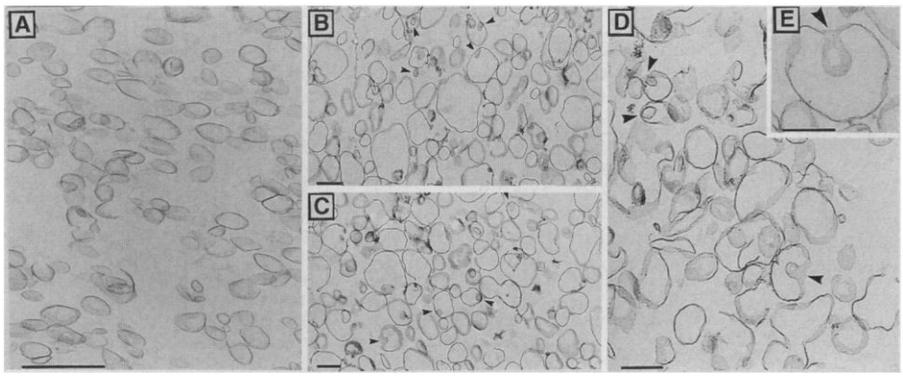

Fig. 2. Electron microscopy of the vesicles (V) purified from the silica-coated rat lung endothelial membranes (**A**) and the detergent-resistant membranes (TI) isolated without silica coating (**B** to **E**). Electron microscopy was performed on membrane isolates as described (*13*). Typical low- and high-power fields are shown. (A) Membranes of the V isolate, showing a homogeneous population of small vesicles with typical caveolar morphology (*13*). Despite the isolation procedure, many caveolae retained their characteristic flask shape. (B to E) Membranes in fraction TI, consisting of many larger vesicles (>150 and <700 nm in diameter) interspersed with smaller caveolar vesicles (<100 nm) and some nonvesiculated, linear membrane sheets. A typical caveola was often apparent attached to the inside of a larger vesicle (arrowheads). Bars, 500 nm (A to D) and 300 nm (E).

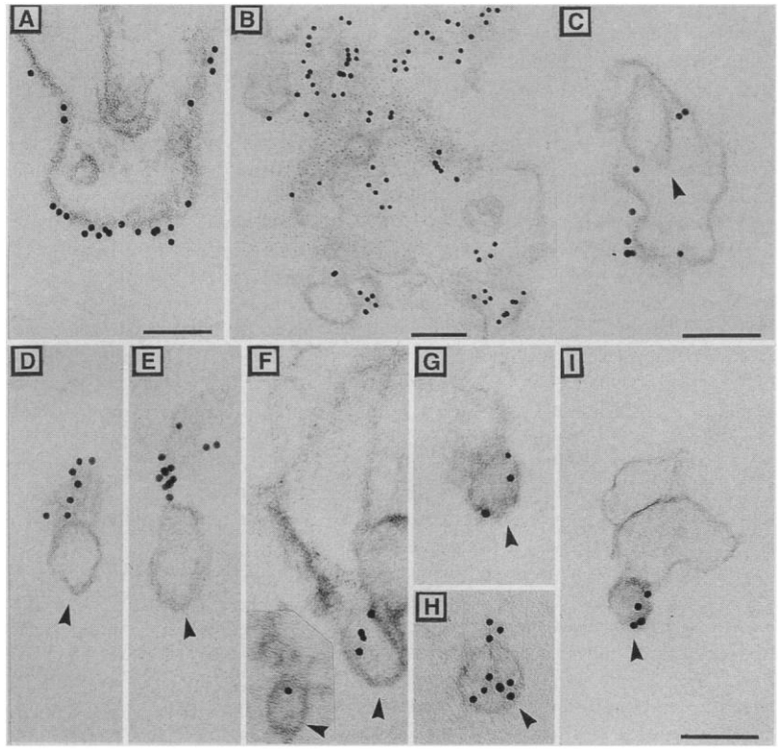

Fig. 3. Colloidal gold localization of CA to large vesicles and G_{M1} to caveolae. Detergent-resistant membrane isolates (TI) were embedded in agarose for gold labeling of CA (**A** to **E**) or G_{M1} (**F** to **I**) (*45, 47*). (A and B) Low-magnification electron micrographs showing immunolabeling of CA. All gold is attached to membranes with little, if any, background labeling. The gold particles are located primarily on the surface of the larger vesicles and some linear membrane sheets, but are not associated with the smaller caveolae. (C to E) Higher magnification images revealing unlabeled caveolae (arrowheads) apparently attached to a large vesicle labeled with gold (C) or associated with labeled membrane strands attached to the neck of the caveolae (D and E). Control experiments with nonimmune serum showed little labeling of membranes; only an occasional gold particle was detected per field examined and appeared equivalent to background labeling of agarose alone. (F to H) Higher magnification micrographs revealing immunogold labeling of G_{M1} inside caveolae (arrowheads), with little labeling of the caveolae-associated larger vesicles (F) or remnant membranes (G). (I) Direct labeling of caveola (arrowhead) with cholera toxin–gold conjugates (*47*). Control experiments performed with conjugates plus a 10-fold molar excess of monomeric cholera toxin showed almost complete absence of gold. Overall, a size criterion was obvious in distinguishing the caveolar vesicles from the larger noncaveolar vesicles. Therefore, we divided the vesicles clearly observed in the electron micrographs into two groups: those with diameters of <80 nm and those with diameters of >150 nm. This size criterion cannot be considered absolute in separating caveolae from noncaveolar vesicles, because, for instance, a few caveolae could remain attached to each other and form a larger vesicle. Nevertheless, 86% of the vesicles of <80 nm were labeled for G_{M1}, with a range of one to nine gold particles per caveola, whereas only 2% were labeled for CA (all labeled with only one gold particle). For the larger vesicles, 80% were labeled for CA and only 13% for G_{M1} (≥50 vesicles were counted in each category). These results support the use of G_{M1} as a caveolar marker, substantiate the size criterion, and are consistent with previous studies on G_{M1} localization (*11, 14*). Bars, 100 nm.

equivalence of this fraction with the immobile fraction detected in the diffusion studies (*33*). Thus, it appears that a substantial but variable fraction of GPI-anchored proteins exists on the cell surface dynamically partitioned into detergent-resistant glycolipid microdomains that are not likely to be simply a consequence of detergent extraction, and that the size of this fraction may depend on cell type, culture, and ligand or antibody exposure.

Normally, and even more so after cross-linking, GPI-anchored proteins can partition into diffusion-restrictive microdomains, some of which may associate with caveolae as an annular region at the opening. Our experiments with detergent-resistant membranes support this model in several ways. Because both domains are resistant to detergent solubilization, the normally flat membrane region surrounding the opening of the caveola is essentially excised from the plasmalemma to form an intact large vesicle with a caveola still attached and located usually inside but sometimes outside of the vesicle. These structures were often detected by electron microscopy (Fig. 2, C to E). The silica coating prevents the coisolation of this microdomain with the caveolae. Consequently, much smaller amounts of GPI-linked proteins were detected in the pure caveola preparations (V) than in preparations containing the larger vesicles (Fig. 1). Indeed, it was the larger vesicles that were rich in GPI-linked proteins, as indicated by both immunoblot analysis (Fig. 1) and immuno-electron microscopy. Immunogold labeling of TI localized CA to the larger vesicles and linear membranes but not the caveolae (Fig. 3, A to C). Consistent with a model of distinct but associated domains, CA was also present on small remnants of plasma membrane outside of the caveolae but still attached to the neck (Fig. 3, D and E). In contrast, immunogold labeling for G_{M1} was frequently detected inside the caveolae (Fig. 3, F to H), consistent with our biochemical data and with gold localization of G_{M1} performed on cells (*11, 14*). In addition, the caveolae were labeled with gold-conjugated cholera toxin (Fig. 3I).

All the membrane subfractions described so far were isolated after exposure to detergent in order to be consistent and limit the number of variables in the comparison of V versus TI versus G. However, the exposure to detergent is of concern. Even though the TI and G preparations require detergent for microdomain excision from the whole membranes, caveolae can be sheared and isolated from P without detergent, although less efficiently (*13, 34*). Caveolin and G_{M1} were enriched in, whereas GPI-anchored proteins were almost completely excluded from, detergent-free purified caveolae (V′) (Fig. 1E).

Lipid anchors such as GPI may control the ability of proteins to partition selectively, but reversibly, within specialized microdomains and, therefore, may subserve a targeting function. The GPI anchor directly affects association with detergent-resistant membranes (*35*), membrane diffusion (*8, 32*), polarized delivery to cell surfaces (*6*), cell activation (*36*), and the rate and pathway of internalization (*10*). Other lipid-anchored proteins, including NRTKs and guanosine triphosphate (GTP)–binding proteins such as Rab5, are found in detergent-resistant complexes (*5, 25, 26, 35, 37*). Our analysis reveals that various NRTKs (Yes and Lyn) (*27*), heterotrimeric GTP-binding proteins (α and $\beta\gamma$ subunits) (*38*), and as yet unidentified small GTP-binding proteins (but not Rab5) (*38*) are indeed present in purified caveolae.

The physical association of GPI-anchored protein microdomains with caveolae suggests functional interplay between them. These structures may provide a platform for ligand processing by integrating signal transduction with membrane transport. Binding of natural ligands or antibodies to GPI-linked proteins can induce clustering (*2, 15*), internalization by caveolae via potocytosis (*21, 39*) or endocytosis (*10, 40, 41*), and even cell activation (*16*). Signaling may regulate caveolar processing (*41, 42*), and various mediators of signaling reside in caveolae (*13, 24, 38*). Lastly, surface-bound molecules are endocytosed or transcytosed by caveolae in endothelium (*14, 18–20, 43*). Disassembly of caveolae prevents such transport (*19*), and molecular mapping of caveolae reveals the presence of SNARE fusion proteins and guanosine triphosphatases necessary for regulated *N*-ethylmaleimide–sensitive vesicular transport (*38, 44*). Caveolae thus appear to contain the molecular machinery for integrating signaling with carrier transport. Dynamic ligand processing via clustering, signaling, and vesicular transport may occur through the association of the GPI-linked protein microdomains with caveolae or even possibly via caveolar formation. Such specialized distinct microdomains may exist separately or associated with each other not only to organize signaling molecules but also to process surface-bound ligands differentially.

REFERENCES AND NOTES

1. T. E. Thompson and T. W. Tillack, *Annu. Rev. Biophys. Biophys. Chem.* **14**, 361 (1985).
2. R. Schroeder, E. London, D. Brown, *Proc. Natl. Acad. Sci. U.S.A.* **91**, 12130 (1994).
3. D. Brown and J. K. Rose, *Cell* **68**, 533 (1992).
4. M. Letarte-Muirhead, R. T. Acton, A. F. Williams, *Biochem. J.* **143**, 51 (1974); D. Hoessli and E. Rungger-Brandle, *Exp. Cell Res.* **156**, 239 (1985); N. M. Hooper and A. J. Turner, *Biochem. J.* **250**, 865 (1988).
5. M. Sargiacomo, M. Sudol, Z. Tang, M. P. Lisanti, *J. Cell Biol.* **122**, 789 (1993); M. P. Lisanti, Z. Tang, M. Sargiacomo, *ibid.* **123**, 595 (1993).
6. D. Brown, B. Crise, J. K. Rose, *Science* **245**, 1499 (1989); K. Simons and G. van Meer, *Biochemistry* **27**, 6197 (1988); M. Garcia, C. Mirre, A. Quaroni, H. Reggio, A. Le Bivic, *J. Cell Sci.* **104**, 1281 (1993).
7. T. V. Kurzchalia *et al.*, *J. Cell Biol.* **118**, 1003 (1992); P. Dupree, R. G. Parton, G. Raposo, T. V. Kurchalia, K. Simons, *EMBO J.* **12**, 1597 (1993).
8. L. A. Hannan, M. P. Lisanti, E. Rodriguez-Boulan, M. Edidin, *J. Cell Biol.* **120**, 353 (1993).
9. K. G. Rothberg, Y. Ying, J. F. Kolhouse, B. A. Kamen, R. G. W. Anderson, *ibid.* **110**, 637 (1990); Y. Ying, R. G. W. Anderson, K. G. Rothberg, *Cold Spring Harbor Symp. Quant. Biol.* **57**, 593 (1992); U. S. Ryan, P. L. Whitney, J. W. Ryan, *J. Appl. Physiol.* **53**, 914 (1982); A. Stahl and B. M. Mueller, *J. Cell Biol.* **129**, 335 (1995).
10. E.-A. Keller, M. W. Siegel, I. W. Caras, *EMBO J.* **3**, 863 (1992).
11. R. G. Parton, *J. Histochem. Cytochem.* **42**, 155 (1994).
12. K. G. Rothberg *et al.*, *Cell* **68**, 673 (1992).
13. J. E. Schnitzer, P. Oh, B. S. Jacobson, A. M. Dvorak, *Proc. Natl. Acad. Sci. U.S.A.* **92**, 1759 (1995).
14. R. Montesano, J. Roth, A. Robert, L. Orci, *Nature* **296**, 651 (1982).
15. S. Mayor, K. G. Rothberg, F. R. Maxfield, *Science* **264**, 1948 (1994).
16. L. F. Thompson, J. M. Ruedi, A. Glass, M. G. Low, A. H. Lucas, *J. Immunol.* **143**, 1815 (1989); P. E. Korty, C. Brando, E. M. Shevach, *ibid.* **146**, 4092 (1991); L. S. Davies, S. S. Patel, J. P. Atkinson, P. E. Lipsky, *ibid.* **141**, 2246 (1988).
17. I. Stefanova, V. Horejsi, I. Ansotegui, W. Knapp, H. Stockinger, *Science* **254**, 1016 (1991); A. M. Shenoy-Scaria *et al.*, *J. Immunol.* **149**, 3535 (1992); P. M. Thomas and L. E. Samelson, *J. Biol. Chem.* **267**, 12317 (1992); T. Cinek and V. Horejsi, *J. Immunol.* **149**, 2262 (1992).
18. J. E. Schnitzer, *Trends Cardiovasc. Med.* **3**, 124 (1993).
19. ———, P. Oh, E. Pinney, J. Allard, *J. Cell Biol.* **127**, 1217 (1994).
20. J. E. Schnitzer and P. Oh, *J. Biol. Chem.* **269**, 6072 (1994); A. J. Milici, N. E. Watrous, H. Stukenbrok, G. E. Palade, *J. Cell Biol.* **105**, 2603 (1987).
21. R. G. W. Anderson, B. A. Kamen, K. G. Rothberg, S. W. Lacey, *Science* **255**, 410 (1992).
22. When cells are isolated from tissues and grown in culture, there can be a substantial loss of caveolae from the cell surface, especially for endothelial cells [J. E. Schnitzer, A. Siflinger-Birnboim, P. J. Del Vecchio, A. B. Malik, *Biochem. Biophys. Res. Commun.* **199**, 11 (1994)]. Such losses (often >100-fold) represent a substantial alteration in plasma membrane organization and may reflect a major perturbation in caveolar function and even GPI-linked protein clustering.
23. B. S. Jacobson, J. E. Schnitzer, M. McCaffery, G. E. Palade, *Eur. J. Cell Biol.* **58**, 296 (1992).
24. T. Fujimoto, S. Nakade, A. Miyawaki, K. Mikoshiba, K. Ogawa, *J. Cell Biol.* **119**, 1507 (1992); T. J. Fujimoto, *ibid.* **120**, 1147 (1993).
25. W.-J. Chang *et al.*, *ibid.* **126**, 127 (1994).
26. M. P. Lisanti *et al.*, *ibid.*, p. 111.
27. J. E. Schnitzer, D. P. McIntosh, P. Oh, unpublished data.
28. L. K. Chaney and B. S. Jacobson, *J. Biol. Chem.* **258**, 10062 (1983); W. F. Patton, M. R. Dhanak, B. S. Jacobson, *Electrophoresis* **11**, 79 (1990).
29. Isolation of caveolae was performed under high-salt conditions to minimize the electrostatic interaction between the cationic silica particles and the polyanionic cell surface. Under these conditions, intact membranes were separated from the silica pellicle, and, with the addition of Triton X-100, low density, detergent-resistant membranes were isolated as usual by sucrose density gradient centrifugation (*13*). GPI-linked proteins not normally associated with pure caveolae, such as 5′-NT, were now present in this isolate (*27*). Furthermore, electron microscopy revealed that the specimens, which appeared biochemically impure by this criterion, contained caveolae mixed with larger vesicular structures, including single caveolae attached to the inside of the larger vesicles, similar to those present in TI (Fig. 2).

30. A. M. Fra, E. Williamson, K. Simons, R. G. Parton, *J. Biol. Chem.* **269**, 30745 (1994); A. Gorodinsky and D. A. Harris, *J. Cell Biol.* **129**, 619 (1995).
31. We do not wish to imply that GPI-anchored proteins can never enter caveolae. Antibody–cross-linked alkaline phosphatase clusters and slowly enters caveolae for endocytosis to endosomes and lysosomes (*41*), consistent with our studies of internalization of modified albumins by caveolae, with the exception that the process of binding, clustering, internalization, and degradation was much quicker for the albumins (*19, 43*). It appears that cell surface processing, at least for GPI-linked proteins, probably comprises three distinct sequential steps: (i) induced movement of GPI-anchored proteins (probably by a ligand) into microdomains near the caveolae, thereby increasing the local concentration of GPI-linked proteins by direct sequestration of previously free molecules or possibly by assembly of several smaller clusters; (ii) eventual movement into the caveolae; and (iii) fission or budding of the caveolae from the membrane for potocytosis or endocytosis.
32. F. Zhang *et al., J. Cell Biol.* **115**, 75 (1991); F. Zhang *et al., Proc. Natl. Acad. Sci. U.S.A.* **89**, 5231 (1992).
33. Specialized glycolipid domains are resistant to detergent extraction and are necessary for maintaining detergent-resistant clusters of GPI-linked proteins (*2–5*). Removal of cholesterol from plasma membranes can dissociate or prevent the formation of such clusters and assure a random, free distribution of GPI-anchored proteins (*39*). As expected, cholesterol removal reduces the resistance of GPI-linked proteins to detergent solubilization (*5*), consistent with the notion that the freely diffusing GPI-anchored proteins are indeed more readily solubilized by detergents than the less mobile GPI-anchored proteins in the glycolipid domains. Moreover, in the absence of glycolipids, GPI-anchored proteins are readily solubilized from membranes by cold Triton X-100; solubility decreases with the addition of appropriate glycolipids (*2*). Thus, GPI-anchored proteins randomly distributed at the cell surface should be susceptible to detergent extraction; indeed, our percentages agree with those from the diffusion studies discussed in the text. In homogenates of non–silica-coated rat lung, ~60% of CA and 75% of 5′-NT are solubilized by Triton X-100 at 4°C. Moreover, mass balances performed on the silica-coated membranes showed that ~20% of 5′-NT and 40% of CA could be isolated in the intact, detergent-resistant membrane fraction TI.
34. As noted in (*13*), caveolae can be isolated without exposure to Triton X-100, but less efficiently. The usual protocol was followed for caveolae isolation, with the exception that Triton X-100 was omitted and, for shearing purposes, the number of homogenization strokes was increased to 48 to 60 from 12.
35. W. Rodgers, B. Crise, J. K. Rose, *Mol. Cell. Biol.* **14**, 5384 (1994).
36. B. Su, G. L. Waneck, R. A. Flavell, A. L. M. Bothwell, *J. Cell Biol.* **112**, 377 (1991).
37. G. Arreaza, K. A. Melkonian, M. LaFevre-Bernt, D. Brown, *J. Biol. Chem.* **269**, 19123 (1994); A. M. Shenoy-Scaria *et al., J. Cell Biol.* **126**, 353 (1994).
38. J. E. Schnitzer, J. Liu, P. Oh, *J. Biol. Chem.* **270**, 14399 (1995).
39. K. G. Rothberg, Y.-S. Ying, B. A. Kamen, R. G. W. Anderson, *J. Cell Biol.* **111**, 2931 (1990).
40. A. Bamezai, V. S. Goldmacher, K. L. Rock, *Eur. J. Immunol.* **22**, 15 (1992).
41. R. G. Parton, B. Joggerst, K. Simons, *J. Cell Biol.* **127**, 1199 (1994).
42. E. J. Smart, D. C. Foster, Y.-S. Ying, B. A. Kamen, R. G. W. Anderson, *ibid.* **124**, 307 (1994).
43. J. E. Schnitzer, A. Sung, R. Horvat, J. Bravo, *J. Biol. Chem.* **264**, 24544 (1992); J. E. Schnitzer and J. Bravo, *ibid.* **268**, 7562 (1993).
44. J. E. Schnitzer, J. Allard, P. Oh, *Am. J. Physiol.* **37**, H48 (1995).
45. The membrane preparations were processed for immuno–electron microscopy by a modification of a previously described procedure [P. De Camilli, S. M. Harris Jr., W. B. Huttner, P. J. Greengard, *J. Cell Biol.* **96**, 1355 (1983)]. The detergent-resistant membranes from rat lung (TI) isolated as described (*26*) directly in suspension from the sucrose gradient were mixed with 4% agarose (Seaplaque; FMC Bioproducts) in phosphate-buffered saline (PBS) at 37°C at a vesicle:agarose volume ratio of 1:3. The suspension was transferred by capillary action into a frame prepared from two glass slides separated at each end by two cover slips (0.17 mm thick). After cooling immediately to solidify the agarose, the frame was removed and the agarose cut into 2-mm squares, which were then incubated in 5% ovalbumin in PBS for 30 min, washed briefly in PBS, and incubated with anti-CA, anti-G_{M1}, or nonimmune serum overnight at 4°C. After five 10-min washes in PBS, the blocks were incubated for 8 hours at 4°C with colloidal gold particles (10 to 15 nm in diameter) conjugated with goat antibodies to rabbit immunoglobulin G. After five 30-min washes in PBS, the agarose-embedded membranes were fixed for 30 min with 1% glutaraldehyde in PBS, washed in 0.1 M sodium cacodylate buffer (pH 7.4) (two times, 5 min each), incubated for 1 hour with 1% OsO_4, dehydrated, and embedded in Epon. Ultrathin sections were cut, stained with 1% lead citrate, and viewed under a Philips P-300 electron microscope.
46. The silica-coated membrane pellet already stripped of caveolae (P–V) was resuspended in 20 mM 2-(*N*-morpholino)ethanesulfonic acid with 125 mM NaCl and an equal volume of 4 M K_2HPO_4 and 0.2% polyacrylate (pH 9.5). The solution was sonicated (10 10-s bursts) with cooling, mixed on a rotator for 8 hours at room temperature (20° to 25°C), and sonicated again (five 10-s bursts). Triton X-100 was added to 1%, and the preparation was then mixed for 10 min at 4°C and homogenized with a Type AA Teflon tissue grinder (Thomas Scientific, Swedesboro, NJ). Any intact floating detergent-resistant membranes were separated and isolated from this homogenate by sucrose density gradient centrifugation as in (*13*). The pellet, containing silica and any remaining membranes, was also collected.
47. Cholera toxin B fragment (CT) at 60 μg/ml was conjugated to 15-nm colloidal gold in 2 mM sodium borate buffer (pH 6.9) for 30 min with stirring. Polyethylene glycol (20 kD) was added for the last 5 min to a final concentration of 0.5 mg/ml. Unconjugated CT was removed by three cycles of centrifugation (10,000*g* for 20 min) and resuspension in 5 mM sodium phosphate buffer (pH 7.2). The resuspended conjugate (CT-Au) was dialyzed overnight against a solution containing 50 mM tris (pH 6.9) and 150 mM NaCl. Sodium azide was added to 0.02% and the conjugate was stored at 4°C. The isolated membranes were labeled as described (*45*), with the exception that CT-Au replaced the primary antibody and was followed directly by washing without additional incubations.
48. We thank J. P. Luzio for providing the antibodies to 5′-NT and W. S. Sly for the polyclonal antibodies to CA. Supported by NIH grants HL43278 and HL52766 (J.E.S.) and AI33372 (A.M.D.), and an Established Investigator Award from the American Heart Association and Genentech (J.E.S.).

12 January 1995; accepted 10 July 1995

Elongin (SIII): A Multisubunit Regulator of Elongation by RNA Polymerase II

Teijiro Aso, William S. Lane, Joan Weliky Conaway, Ronald C. Conaway*

The Elongin (SIII) complex activates elongation by mammalian RNA polymerase II by suppressing transient pausing of the polymerase at many sites within transcription units. Elongin is a heterotrimer composed of A, B, and C subunits of 110, 18, and 15 kilodaltons, respectively. Here, the mammalian Elongin A gene was isolated and expressed, and the Elongin (SIII) complex reconstituted with recombinant subunits. Elongin A is shown to function as the transcriptionally active component of Elongin (SIII) and Elongin B and C as regulatory subunits. Whereas Elongin C assembles with Elongin A to form an AC complex with increased specific activity, Elongin B, a member of the ubiquitin-homology gene family, appears to serve a chaperone-like function, facilitating assembly and enhancing stability of the Elongin (SIII) complex.

Eukaryotic messenger RNA synthesis is a complex biochemical process controlled in part by the concerted action of a set of general transcription factors that regulate the activity of RNA polymerase II (Pol II) at both the initiation and elongation stages of transcription. At least six general initiation factors (TFIIA, TFIIB, TFIID, TFIIE, TFIIF, and TFIIH) have been identified in eukaryotic cells and found to promote selective binding of RNA polymerase II to promoters and to support a basal level of transcription (*1*).

In addition to the general initiation factors, three general elongation factors [SII, TFIIF, and Elongin (SIII)] from eukaryotes have been defined biochemically and shown to increase the overall rate at which Pol II transcribes duplex DNA (*2–4*). SII is an ~38-kD elongation factor (*5*) that promotes passage of Pol II through transcriptional impediments such as nucleoprotein complexes and DNA sequences that act as intrinsic arrest sites. SII-dependent readthrough is accompanied by reiterative transcript cleavage and reextension of nascent transcripts held in the Pol II active site (*6–9*).

TFIIF from higher eukaryotes is a heterodimer composed of ~70-kD (RAP74)

T. Aso, J. W. Conaway, R. C. Conaway, Program in Molecular and Cell Biology, Oklahoma Medical Research Foundation, 825 Northeast 13th Street, Oklahoma City, OK 73104, USA.
W. S. Lane, Harvard Microchemistry Facility, Harvard University, 16 Divinity Avenue, Cambridge, MA 02138, USA.
* To whom correspondence should be addressed.